

Endothelial but not systemic ferroptosis inhibition protects from antineutrophil cytoplasmic antibody–induced crescentic glomerulonephritis



OPEN

Anthony Rousselle¹, Dörte Lodka¹, Janis Sonnemann^{1,2}, Lovis Kling^{1,2}, Ralph Kettritz^{1,2} and Adrian Schreiber^{1,2}

¹Experimental and Clinical Research Center, Max Delbrück Center for Molecular Medicine (MDC) and Charité—Universitätsmedizin Berlin, Corporate Member of Freie Universität Berlin and Humboldt-Universität zu Berlin, Berlin, Germany; and ²Department of Nephrology and Medical Intensive Care Medicine, Charité-Universitätsmedizin Berlin, Berlin, Germany

Antineutrophil cytoplasmic antibody (ANCA)-associated vasculitides (AAV) are systemic autoimmune diseases featuring small blood vessel inflammation and organ damage, including necrotizing crescentic glomerulonephritis (NCGN). Persistent vascular inflammation leads to endothelial and kidney cell necrosis. Ferroptosis is a regulated cell death pathway executed by reactive oxygen species and iron-dependent lipid peroxidation culminating in cell membrane rupture. Here we show that ANCA-activated neutrophils induced endothelial cell (EC) death *in vitro* that was prevented by ferroptosis inhibition with Ferrostatin-1, Liproxstatin-1 and small inhibiting RNA against the enzyme AcylCoA Synthetase Long Chain Family Member 4 (ACSL4). In contrast, neither necroptosis nor apoptosis inhibition affected EC death. Moreover, both ferroptosis inhibitors alleviated lipid peroxide accumulation in EC. Increased lipid peroxidation was detected in kidney sections of AAV mice by immunohistochemistry. We generated MPO^{-/-} ACSL4^{fllox} Tie2-Cre⁺ mice lacking ACSL4 specifically in EC (ACSL4^{ΔEC}) to study the significance of endothelial ferroptosis *in vivo*. ACSL4^{ΔEC} chimeric mice, but not control mice (ACSL4^{WT}), were protected from NCGN in an MPO-AAV bone-marrow transplantation model. These data establish that EC ferroptosis contributes to ANCA-induced glomerulonephritis. However, systemic pharmacological ferroptosis inhibition with Ferrostatin-1 or Liproxstatin-1 did not protect from NCGN in a murine AAV model. Ferrostatin-1 treatment both directly activated T-cell proliferation and indirectly myeloid-mediated T-cell proliferation and polarization *in vitro*. Conceivably, both effects may cancel the beneficial effect of endothelial ferroptosis inhibition. Mechanistically, we describe the importance of EC ferroptosis for the development of AAV. However, the lack of protection with systemic pharmacological ferroptosis inhibition should discourage

clinicians from evaluating this treatment strategy in clinical AAV studies.

Kidney International (2025) **107**, 1037–1050; <https://doi.org/10.1016/j.kint.2025.02.023>

KEYWORDS: ANCA; endothelial cells; ferroptosis; glomerulonephritis; vasculitis

Copyright © 2025, International Society of Nephrology. Published by Elsevier Inc. This is an open access article under the CC BY license (<http://creativecommons.org/licenses/by/4.0/>).

Translational Statement

We characterized the contribution of endothelial cell ferroptosis in antineutrophil cytoplasmic antibody (ANCA)-associated vasculitis (AAV). ANCA-stimulated neutrophils induced endothelial cell ferroptosis characterized by increased lipid peroxidation. Specific deletion of the ferroptosis mediator ACSL4 in endothelial cells prevented necrotizing crescentic glomerulonephritis in a murine AAV model. In contrast, systemic pharmacologic ferroptosis inhibition showed no protection. In fact, Ferrostatin-1 treatment increased pathogenic pathways, such as T helper 17 cell abundance in kidneys and neutrophil extracellular trap generation. Our findings establish the importance of endothelial ferroptosis for the development of AAV but raise concern about systemic ferroptosis inhibition as a treatment for patients with AAV.

Antineutrophil cytoplasmic antibody (ANCA)-associated vasculitides are systemic autoimmune diseases characterized by inflammation of small blood vessels and multiorgan damage, including necrotizing and crescentic glomerulonephritis (NCGN).^{1,2} ANCA autoantibodies recognize the autoantigens myeloperoxidase (MPO) or proteinase 3 (PR3), exclusively expressed by neutrophil granulocytes and monocytes.³ ANCA bind to their cell surface-presented antigens and activate both myeloid cell types.⁴ Once activated, these cells release several proinflammatory mediators that damage the endothelium and further promote vascular inflammation and cell necrosis.⁵

Correspondence: Adrian Schreiber, Experimental and Clinical Research Center, Lindenberger Weg 80, 13125 Berlin, Germany. E-mail: adrian.schreiber@charite.de

Received 3 June 2024; revised 20 December 2024; accepted 25 February 2025; published online 22 March 2025

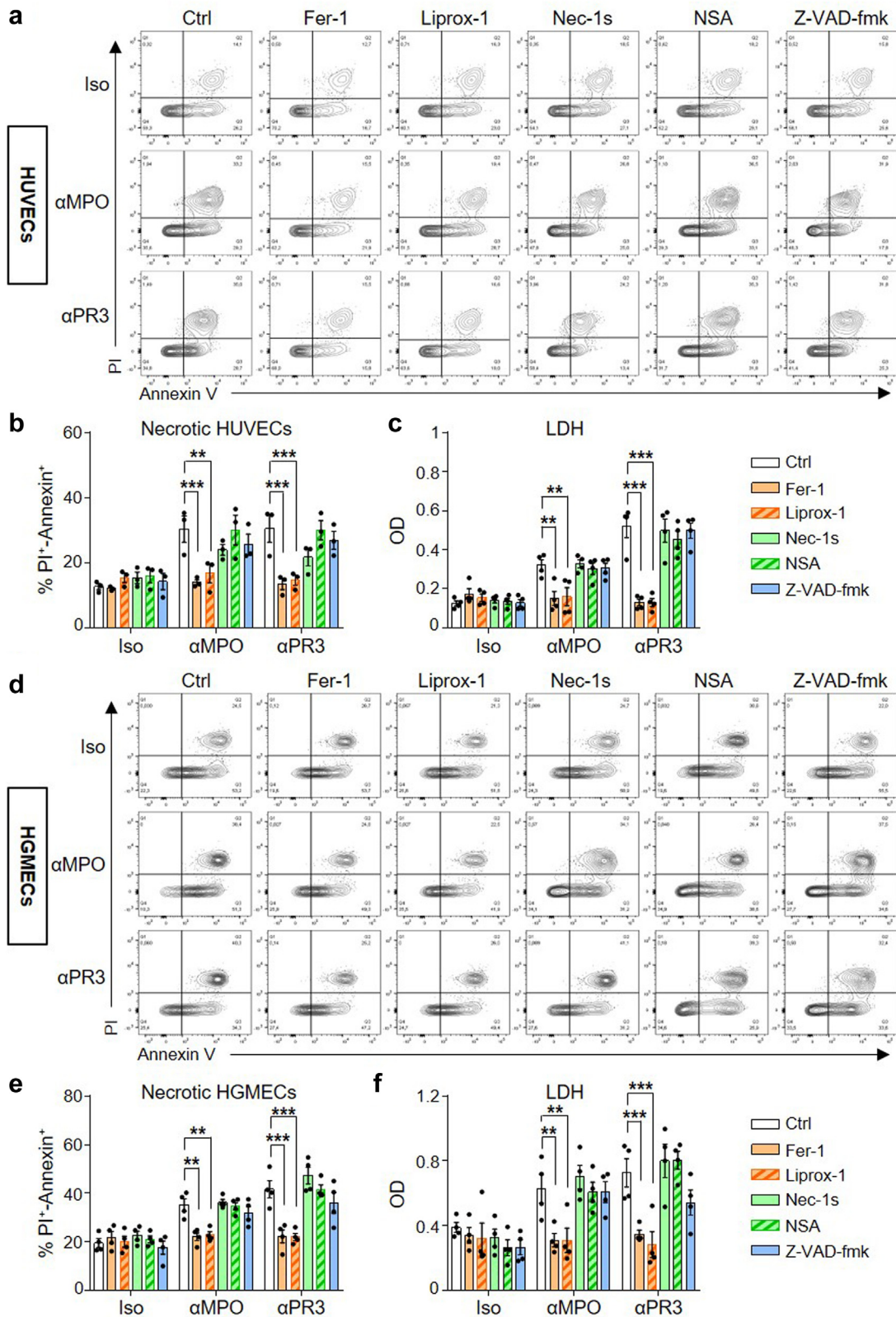


Figure 1 | Cell-free supernatants (cf-SN) from antineutrophil cytoplasmic antibody (ANCA)-stimulated neutrophils induce ferroptosis in human endothelial cells. cf-SN from human neutrophils stimulated with either isotype, anti-myeloperoxidase (anti-MPO), or anti-proteinase 3 (anti-PR3) IgG were added to human umbilical vein endothelial cells (HUVECs) or human glomerular microvascular endothelial cell (HGMECs) for 16 hours. Ferrostatin-1 (Fer-1, 10 μ M) and Liproxstatin (Liprox-1, 10 μ M) were used to inhibit ferroptosis. Necroptosis was inhibited by the addition of Necrostatin-1s (Nec-1s, 10 μ M) and Necrosulfonamide (NSA, 5 μ M). Apoptosis was inhibited with 10 μ M pan-caspase inhibitor Z-VAD-fmk (carbobenzoxy-valyl-alanyl-aspartyl-[O-methyl]-fluoromethylketone). At the end of the experiment, (continued)

Serine proteases and neutrophil extracellular traps (NETs) released from ANCA-activated neutrophils mediate endothelial cell (EC) injury and death.^{6,7}

Necrosis, in contrast to apoptosis, has long been considered as an unregulated cell death. However, several regulated necrotic cell death pathways were characterized over the last 2 decades, including necroptosis and ferroptosis.⁸ Necroptosis is controlled by the pathway dependent on receptor-interacting protein kinase1/3 and mixed-lineage kinase domain-like protein (MLKL) and leads to plasma membrane rupture.⁹ We previously established the importance of necroptosis and NETs for autoimmune NCGN.⁷ Ferroptosis provides a different form of regulated cell death that depends on iron and reactive oxygen species.¹⁰ The subsequent accumulation of lipid peroxides causes cell membrane rupture and release of damage-associated molecular patterns. Lipid peroxidation is mediated by key enzymes, including acyl-CoA synthetase long chain family member 4 (ACSL4).^{11,12} Proteins belonging to the antioxidant system, such as glutathione peroxidase 4 (GPX4), protect cell membranes from peroxidation damage.¹³ Ferroptosis regulates several physiological processes, but its contribution to diseases is still incompletely understood.¹⁴ Ferroptosis in resident kidney cells has been linked to kidney damage in ischemia/reperfusion and nephrotoxic acute kidney injury (AKI).^{15,16} In addition, ferroptosis activation in neutrophils has been implicated in autoimmune disease, namely systemic lupus erythematosus.¹⁷

We hypothesized that ferroptosis would mediate EC death in AAV and that ferroptosis inhibition may therefore represent a new therapeutic option. We establish EC ferroptosis as an important disease mechanism in preclinical AAV models. Importantly, our data support the notion that systemic pharmacologic ferroptosis inhibition does not provide protection from AAV and therefore should not be further explored in clinical studies.

METHODS

Materials

Complete and incomplete Freund's adjuvant, liberase, deoxyribonuclease, fetal bovine serum, phorbol 12-myristate 13-acetate, and Ferrostatin-1 were from Sigma-Aldrich. Ionomycin and necrosulfonamide were purchased from Calbiochem-Merck. Liproxstatin-1 was obtained from Sigma-Aldrich and Selleckchem. Roswell Park Memorial Institute 1640 medium and phosphate-buffered saline without magnesium and calcium ions were from Biochrom GmbH.

HUVECs (human umbilical vein ECs) and HGMECs (primary human glomerular microvascular ECs) were obtained from Sigma-Aldrich and Cell Systems, respectively. Necrostatin-1s were ordered from VWR International GmbH and Z-VAD-fmk from Enzo Life Sciences. Human and mouse tumor necrosis factor- α were from R&D Systems. Anti-MPO monoclonal antibody (clone 2C7) was purchased from OriGene, and anti-PR3 monoclonal antibody (clone 43-8-3) isolated from hybridomas generated by BioGenes GmbH.

Animal experiments

Mice were kept under specific pathogen-free conditions at the Max Delbrück Center for Molecular Medicine animal facility. *Acs14^{Flox}* mice were kindly provided by M. Conrad (Helmholtz Zentrum München, Neuherberg, Germany). B6.Cg-Tg(Tekcre)12Flv/J (Tie2-cre) mice were obtained from the Jackson Laboratory. The purification of murine MPO and the immunization of *Mpo^{-/-}* mice were performed as described previously.¹⁸ In brief, *Mpo^{-/-} × Acs14^{Flox} × Tie2Cre⁺* and *Mpo^{-/-} × Acs14^{Flox} × Tie2Cre⁻* (generated by crossing *Mpo^{-/-}*, *Acs14^{Flox}*, and *Tie2Cre^{+/-}* mice) mice were immunized i.p. with murine MPO in complete Freund's adjuvant, boosted i.p. with murine MPO in incomplete Freund's adjuvant after 4 weeks, lethally irradiated, and subsequently transplanted i.v. with bone marrow cells (1.5×10^7) from C57BL/6J (the Jackson Laboratory) wild-type (WT) mice. Mice were sacrificed 7–8 weeks after transplantation. For the passive transfer model, C57BL/6J mice were treated with granulocyte colony-stimulating factor (30 μ g/mouse) subcutaneously at days 8, 4, and 0, lipopolysaccharide (5 μ g/g body weight) i.p. injection, and α MPO IgG (50 μ g/g body weight) i.v. injection at day 0. Ferroptosis inhibition was mediated by daily i.p. injection of Ferrostatin-1 (Fer-1, 3 μ g/g body weight) or Liproxstatin-1 (Liprox-1, 10 μ g/g body weight) from day 0 until sacrifice at day 7.

The isolation of α MPO IgG from immunized mice was performed as previously described.¹⁸ Male and female mice were used. Animal experiments were approved by the local authorities (Landesamt für Gesundheit und Soziales, Berlin, Germany) and followed the Animal Research: Reporting of In Vivo Experiments (ARRIVE) guidelines.

RESULTS

ANCA-stimulated human neutrophils induce ferroptosis in human endothelial cells

We first activated human neutrophils with ANCA to produce cell-free supernatants (cf-SN). Cells were primed with tumor

Figure 1 | (continued) HUVECs and HGMECs were stained with Annexin V–fluorescein isothiocyanate and propidium iodide (PI) and analyzed by flow cytometry. Necrotic cells defined as Annexin V⁺/PI⁺ cells were quantified (n = 3/4 per condition). (a) Representative FACS plot and (b) quantification showing HUVEC necrosis after incubation with cf-SN from ANCA-stimulated neutrophils and the protective effect of Fer-1 and Liprox-1. In contrast, Nec-1s, NSA, and Z-VAD-fmk had no protective effects. (c) LDH release from HUVECs in culture medium was determined by ELISA. Only ferroptosis inhibitors significantly reduced lactate dehydrogenase (LDH) release. (d) Representative fluorescence-activated cell sorting plot and (e) quantification showing HGMEC necrosis after incubation with cf-SN from ANCA-stimulated neutrophils and the protective effect of Fer-1 and Liprox-1. In contrast, other inhibitors had no protective effects. (f) LDH release from HGMECs in culture medium was determined by enzyme-linked immunosorbent assay. Only ferroptosis inhibitors significantly reduced LDH release. Error bars indicate means \pm SEM. **P < 0.01; ***P < 0.001. Ctrl, control mice; OD, optical density.

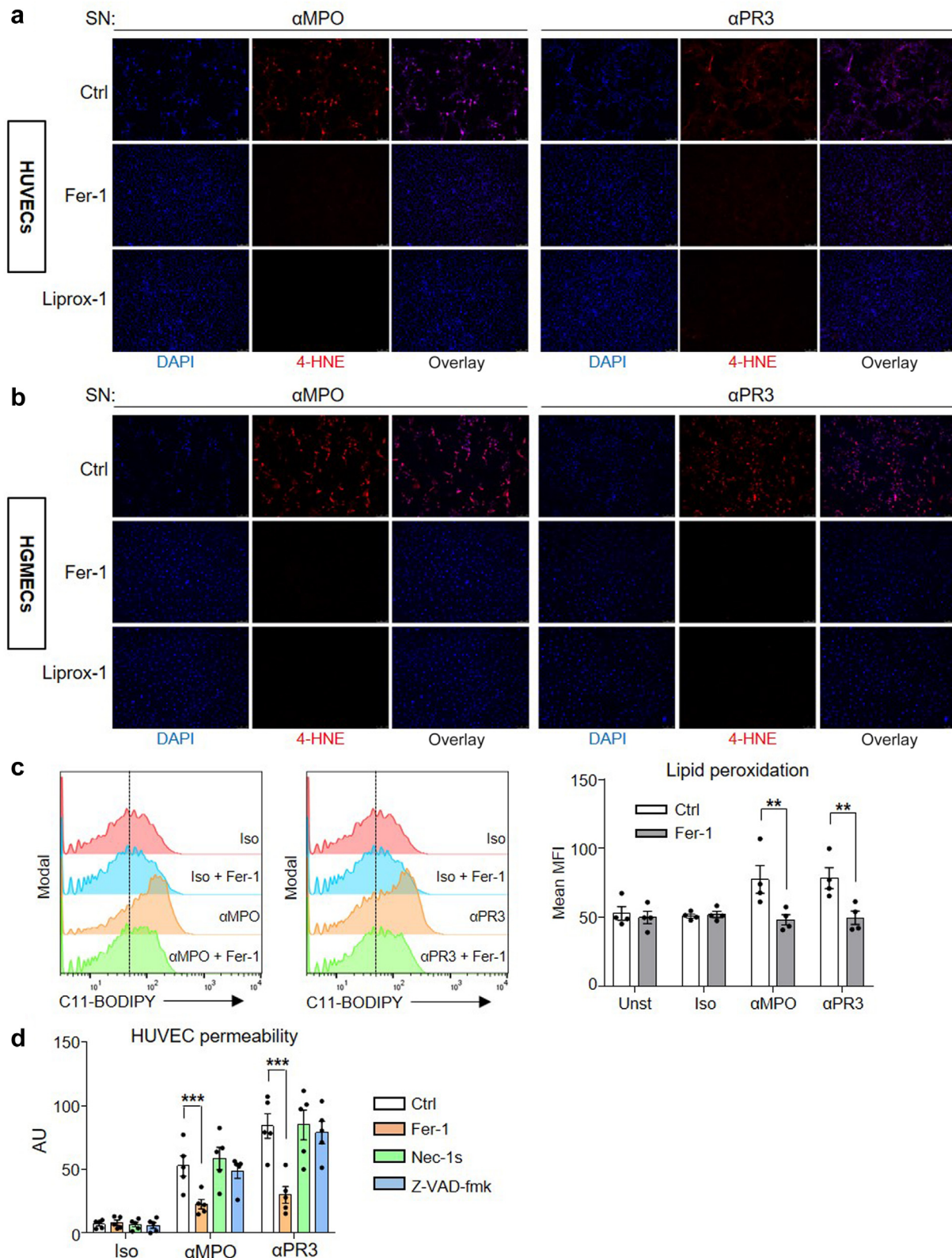


Figure 2 | Cell-free supernatants (cf-SN) from antineutrophil cytoplasmic antibody (ANCA)-stimulated neutrophils increase lipid peroxidation in human endothelial cells. (a) Human umbilical vein endothelial cells (HUVECs) and (b) human glomerular microvascular endothelial cells (HGMECs) were incubated for 16 hours with SN from ANCA-stimulated neutrophils as described in [Supplementary Figure S1A](#). In some conditions, Ferrostatin-1 (Fer-1) and Liproxstatin-1 (Liprox-1) pretreatment were performed to inhibit ferroptosis. Cells were then washed, stained for lipid peroxidation (4-HNE, red) and nuclei (4',6-diamidino-2-phenylindole [DAPI], blue), and observed by microscopy (original magnification $\times 20$). Ferroptosis inhibition significantly reduced the production of the cytotoxic lipid (continued)

necrosis factor- α and stimulated for 2 hours with either α MPO, α PR3, or isotype IgG, respectively. cf-SN were collected and added to confluent HUVECs and HGMECs (Supplementary Figure S1A). cf-SN from neutrophils stimulated with α MPO and α PR3 antibodies induced necrosis in HUVECs (Figure 1a and b) and HGMECs (Figure 1d and e), as illustrated by the increased number of Annexin V/propidium iodide double-positive cells determined by flow cytometry. Different inhibitors of regulated necrosis were added to ECs to dissect which specific cell death pathway was involved. Here, both necroptosis inhibition with Necrostatin-1s or Necrosulfonamide and apoptosis inhibition with caspase inhibitor (Z-VAD-fmk) did not reduce necrosis in HUVECs incubated with supernatants from ANCA-stimulated neutrophils. In contrast, specific ferroptosis inhibition with Fer-1 or Liprox-1 significantly reduced necrosis in HUVECs (Figure 1a and b) and HGMECs (Figure 1d and e). In addition, the release of lactate dehydrogenase, characteristic of a damaged plasma membrane, was significantly reduced by both ferroptosis inhibitors in both HUVECs (Figure 1c) and HGMECs (Figure 1f). We observed no effects using necroptosis and apoptosis inhibitors. We evaluated lipid peroxidation in HUVECs and HGMECs using staining for 4-hydroxynonenal (4-HNE), a reaction product generated during ferroptosis. We observed by microscopy that 4-HNE staining in cells incubated with cf-SN from neutrophils stimulated with α MPO and α PR3 antibodies was increased, whereas cf-SN from neutrophils stimulated with isotype IgG had no effect (Figure 2a and b and Supplementary Figure S1B and C). Ferroptosis inhibition with Fer-1 and Liprox-1 treatment abrogated 4-HNE generation in HUVECs and HGMECs and prevented cell detachment. In addition, we used the lipid peroxidation sensor C11-BODIPY and flow cytometry. Again, we saw increased lipid peroxidation in HUVECs incubated with cf-SN from neutrophils stimulated with α MPO and α PR3 antibodies compared with cf-SN from isotype-stimulated neutrophils (Figure 2c). Fer-1 treatment significantly decreased lipid peroxidation in HUVECs. We speculated that ferroptosis in HUVECs would compromise the endothelial barrier. Indeed, we observed that cf-SN from α MPO- and α PR3-stimulated neutrophils increased trans-endothelial albumin flux through a HUVEC monolayer (Figure 2d). This effect was significantly reduced by Fer-1 treatment but not by Necrostatin-1s nor Z-VAD-fmk treatment. cf-SN from neutrophils stimulated with isotype IgG or inhibitors alone did not perturb the integrity of the HUVEC barrier (Figure 2d). As a complementary strategy to Fer-1 and

Liprox-1 treatment, we used small, interfering RNA (siRNA) against ACSL4, an important mediator of lipid peroxidation, to inhibit ferroptosis. HUVEC transfection with siRNA against ACSL4 reduced the ACSL4 protein level by approximately 75% compared with scramble siRNA (Figure 3a). Importantly, siRNA against ACSL4 significantly reduced HUVEC necrosis in response to cf-SN from neutrophils stimulated with α MPO and α PR3 antibodies when compared with scramble siRNA (Figure 3b and c). We further used this siRNA approach to target MLKL and interfere with the necroptosis pathway. siRNA against MLKL decreased the MLKL protein level by approximately 60% in HUVECs compared with scramble siRNA (Figure 3d). In contrast to ACSL4, MLKL knockdown had no effect on HUVEC necrosis induced by cf-SN from neutrophils stimulated with α MPO and α PR3 antibodies. These data confirm that necroptosis is not induced in ECs incubated with neutrophil cf-SN (Figure 3e and f). Altogether, these results demonstrate that cf-SN from ANCA-stimulated neutrophils induce ferroptosis in EC, thereby compromising the endothelial barrier.

Ferroptosis is activated in kidneys from mice with AAV

Next, we studied whether ferroptosis was increased in kidneys from mice with α MPO-induced NCGN using a preclinical AAV mouse model. We stained kidney sections for 4-HNE, a lipid peroxidation marker, and CD31 as an EC marker. In control mice, we observed bright CD31 staining in glomeruli and tubulointerstitial vessels and only a weak background 4-HNE staining (Figure 4a). In contrast, the 4-HNE signal was increased in AAV mice. The localization pattern of 4-HNE staining was glomerular, periglomerular, and extraglomerular vessels. Some glomeruli preserved CD31 staining, whereas others lacked CD31⁺ cells as the consequence of EC damage. Additional ferroptosis markers, such as CD71 and malondialdehyde, confirmed these data as they were increased in kidneys from AAV mice compared with control mice (Supplementary Figure S2). When we analyzed protein levels of GPX4 and ACSL4 in kidney lysates by western blot, we observed that ACSL4 protein was notably upregulated, whereas GPX4 was strongly reduced in mice with AAV compared with control mice (Figure 4b and c). Quantitative reverse transcriptase–polymerase chain reaction analyses for *Acs4* and *Gpx4* genes showed a similar regulation pattern at mRNA levels (Figure 4d and e). Mechanistically, these results suggest that the increased ferroptosis observed in kidneys from AAV mice resulted

Figure 2 | (continued) oxidation product 4-hydroxynonenal (4-HNE). A representative image for each condition is shown (from $n = 3$ experiments). Bar = 100 μ m. (c) cf-SN were added to HUVECs for 16 hours. Fer-1 (10 μ M) was used to inhibit ferroptosis. At the end of the experiment, HUVECs were stained with C11-BODIPY 581/591 and analyzed by flow cytometry ($n = 4$ per condition). A representative FACS plot showing lipid peroxidation in HUVECs after incubation with cf-SN from ANCA-stimulated neutrophils and the protective effect of Fer-1 is presented. (d) Increased HUVEC permeability by cf-SN from alpha myeloperoxidase (α MPO) and alpha proteinase 3 (α PR3) mAb-stimulated neutrophils. Ferroptosis inhibition with Fer-1 significantly reduced endothelial cell permeability, whereas neither necroptosis inhibition with Nec-1s nor apoptosis inhibition with Z-VAD-fmk exerted beneficial effects ($n = 5$ per condition). Error bars indicate means \pm SEM. ** $P < 0.01$; *** $P < 0.001$. AU, arbitrary unit; Ctrl, control mice; FACS, fluorescence-activated cell sorting; Iso, isotype; MFI, mean fluorescence intensity. To optimize viewing of this image, please see the online version of this article at www.kidney-international.org.

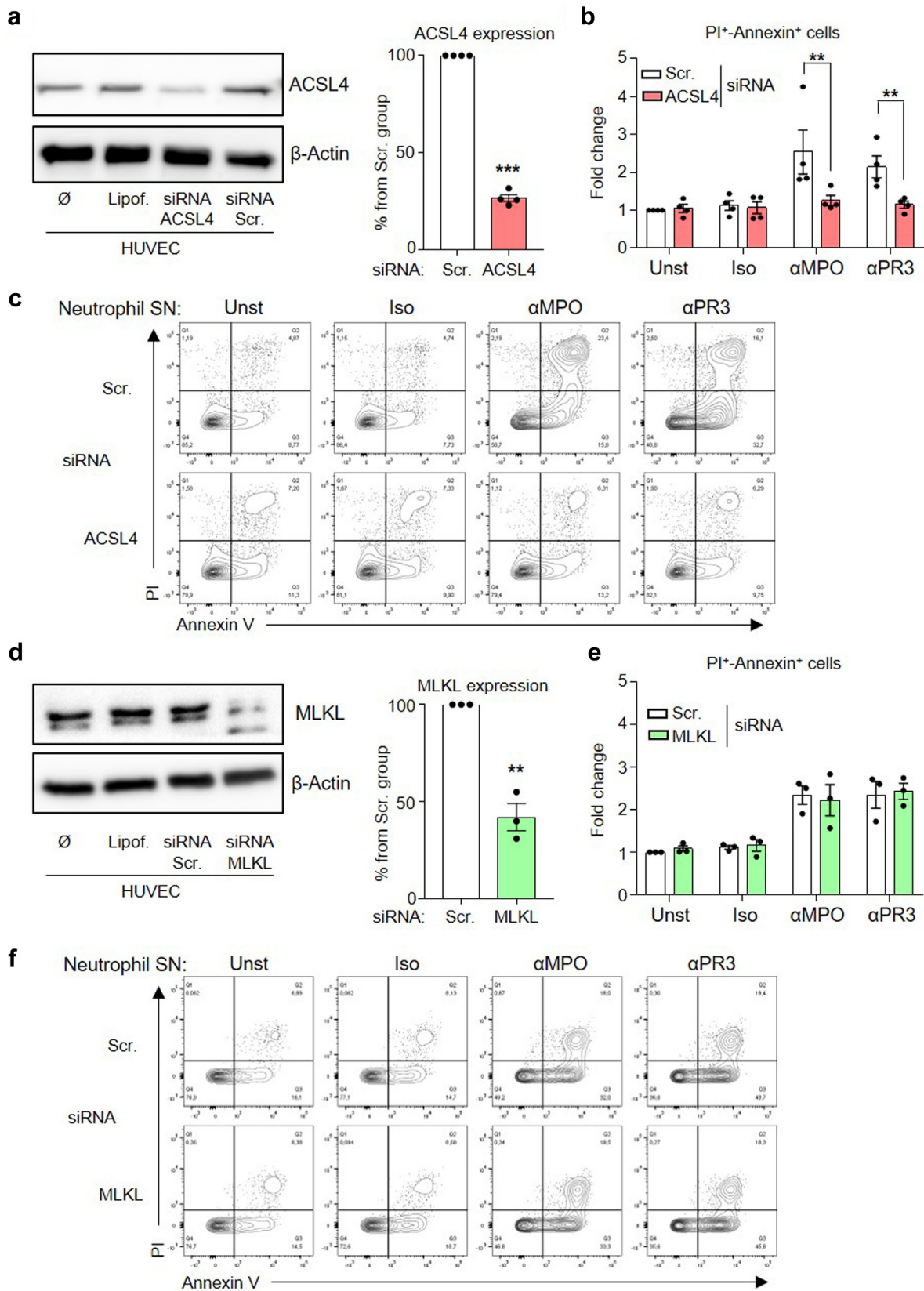


Figure 3 | Acyl-CoA synthetase long chain family member 4 (ACSL4), but not mixed-lineage kinase domain-like protein (MLKL), knockdown decreases endothelial cell death induced by supernatants from antineutrophil cytoplasmic antibody (ANCA)-stimulated neutrophils. (a) Human umbilical vein endothelial cells (HUVECs) were transfected with either small, interfering RNA (siRNA) directed against ACSL4 or scrambled siRNA. HUVECs with and without Lipofectamine (Lipof.) were used as controls. A representative western blot (continued)

from an increased expression of the pro-ferroptotic ACSL4 protein together with a decreased expression of the anti-ferroptotic GPX4 protein.

Chimeric mice lacking ACSL4 in endothelial cells are protected from anti-MPO IgG-induced NCGN

To assess the contribution of EC ferroptosis to AAV, we generated mice with an EC-specific ACSL4 deletion. For this purpose, we bred ACSL4^{lox}, MPO^{-/-} and Tie2-Cre⁺ mice to obtain MPO^{-/-} ACSL4^{lox} Tie2-Cre⁺ (Acsl4^{ΔEC}) mice deficient for ACSL4 in EC only and Tie2-Cre⁻ (Acsl4^{WT}) littermate control mice. We immunized both mouse lines with murine MPO to induce the production of anti-MPO immunity. Mice were then irradiated and transplanted with bone marrow cells from WT mice. Animals were sacrificed 7–8 weeks after transplantation (Figure 5a), and urine, serum, and kidneys were analyzed. Kidney histology revealed protection from kidney damage in Acsl4^{ΔEC} mice with a significantly reduced percentage of crescentic and necrotic glomeruli compared with Acsl4^{WT} mice (Figure 5b). In accordance with that, we detected reduced malondialdehyde signal by immunohistochemistry and microscopy in Acsl4^{ΔEC} compared with Acsl4^{WT} mice (Figure 5c). The urine albumin/creatinine ratio was similar in both groups (Figure 5d), and urinary neutrophil gelatinase-associated lipocalin was decreased in Acsl4^{ΔEC} mice, albeit not significantly (Figure 5e). Analyzing renal infiltrating myeloid cells by flow cytometry, we detected similar numbers of infiltrating CD11b⁺Ly6C^{hi} inflammatory monocytes and CD11b⁺Ly6G⁺ neutrophils in both groups (Figure 5f).

These results from a genetic model strongly establish that EC ferroptosis mediates AAV development in mice. Moreover, these findings suggest that pharmacologic ferroptosis inhibition represents a potential therapeutic strategy for patients with AAV. We next tested this hypothesis in a preclinical murine AAV model.

Ferroptosis inhibition with Fer-1 and Liprox-1 does not protect mice from ANCA-associated NCGN

We used a passive AAV mouse model to investigate the effects of Fer-1 and Liprox-1 treatment *in vivo*. C57Bl/6J mice received granulocyte colony-stimulating factor, lipopolysaccharide, and anti-MPO IgG at the indicated time points (Figure 6a, Supplementary Figure S3A). One group of mice received daily injection of Fer-1 or Liprox-1 from disease initiation at day 0 until sacrifice at day 7. Another group of mice was treated with buffer only and served as control. An additional group of healthy mice was included to provide

baseline values for the different analyzed parameters. In contrast to our hypothesis, ferroptosis inhibition did not protect mice from AAV-associated NCGN. Fer-1-treated and control mice developed similar percentage of glomeruli with crescent and necrosis (Figure 6b). Similar observations were made in mice treated with Liprox-1 (Supplementary Figure S3B). Regarding lipid peroxidation, the malondialdehyde signal detected by immunohistochemistry and microscopy was not modified by Fer-1 treatment (Supplementary Figure S4A) as were urine albumin/creatinine ratio and neutrophil gelatinase-associated lipocalin levels by both treatments (Figure 6c, Supplementary Figure S3C and D). Moreover, the number of kidney-infiltrating CD11b⁺Ly6G⁺ neutrophils and CD11b⁺Ly6C^{hi} inflammatory monocytes detected by flow cytometry was not affected by Fer-1 and Liprox-1 treatment (Figure 6e, Supplementary Figure S3E). In addition to innate immune cells, we assessed T-cell subsets that were shown to mediate kidney injury in AAV. We detected a similar percentage of renal CD4⁺ cells in the Fer-1 treatment and control group but observed differences in the T-cell helper (T_H) subset composition (Figure 6f and Supplementary Figure S4B). IFNγ⁺ T_H1 cells represented the prominent subset and numbers were similar in both groups. In contrast, IL17A⁺ T_H17 cells were significantly increased in mice treated with Fer-1.

These results reject our hypothesis and strongly suggest that systemic pharmacologic ferroptosis inhibition does not represent a therapeutic option for AAV. A question that arises from these findings pertains to mechanisms of how Fer-1 modulates T-cell proliferation and/or polarization. We did several exploratory experiments to gain first insight into potential explanations for the lacking protection of systemic Fer-1 treatment. We focused on CD4⁺ T cells, monocytes, and neutrophils because these cells were shown to contribute to AAV.

Ferroptosis inhibition modulates T-cell proliferation, monocyte-mediated T_H17 polarization, and NET release

First, we investigated whether ferroptosis was modulated in activated CD4⁺ T cells *in vitro*. Murine cells isolated from spleens were incubated in the presence or absence of T-cell activating CD3/CD28 Dynabeads. After 3 days in culture, we evaluated lipid peroxidation in CD4⁺ T cells using the lipid peroxidation sensor C11-BODIPY and flow cytometry. Compared with cells cultured without Dynabeads, lipid peroxidation in activated cells was increased (Figure 7a). Fer-1 treatment abrogated this effect, suggesting that ferroptosis is induced during CD4⁺ T-cell activation. We then questioned

Figure 3 | (continued) showing efficient ACSL4 knockdown is shown (n = 4). β-Actin was used as loading control. **(b)** HUVECs transfected with either a scramble siRNA or siRNA against ACSL4 were incubated with cell-free supernatants from neutrophils stimulated with alpha myeloperoxidase (αMPO), alpha proteinase 3 (αPR3), or isotype IgG for 16 hours. HUVECs were stained with Annexin V–fluorescein isothiocyanate and propidium iodide (PI) and analyzed by flow cytometry. Necrotic cells defined as Annexin V⁺/PI⁺ cells were quantified (n = 4 per condition). **(c)** A representative flow cytometry plot is shown for each condition. **(d)** HUVECs were transfected with either siRNA directed against MLKL or scrambled siRNA. HUVECs with and without Lipof. were used as controls. A representative western blot showing efficient MLKL knockdown is shown (n = 3). β-Actin was used as loading control. **(e)** HUVECs were treated and analyzed as described above (n = 3 per condition). **(f)** A representative flow cytometry plot is shown for each condition. Error bars indicate means ± SEM. **P < 0.01; ***P < 0.001.

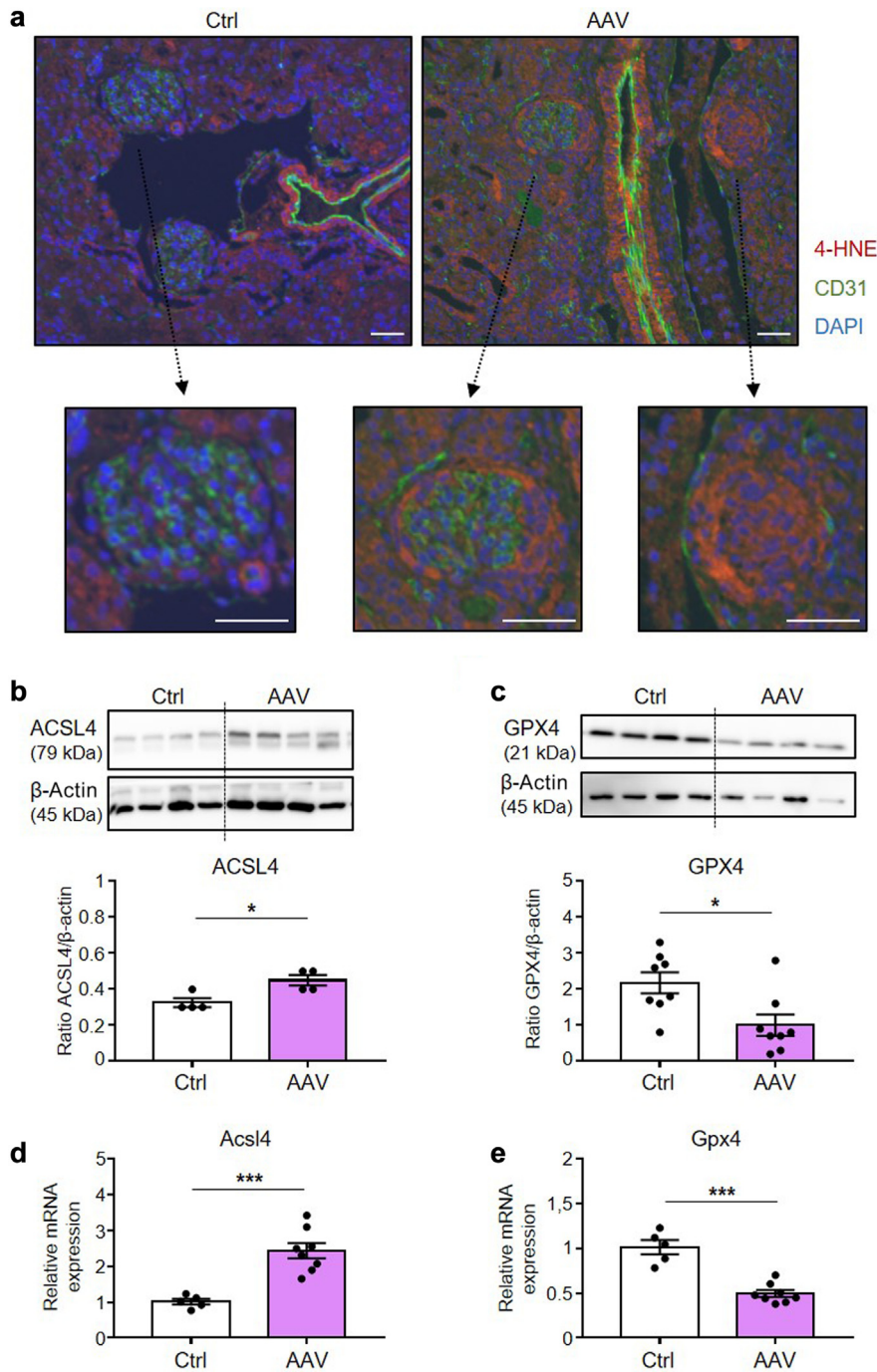


Figure 4 | Ferroptosis is activated in kidneys from mice with antineutrophil cytoplasmic antibody-associated vasculitis (AAV). (a) Representative immunofluorescence images for 4-hydroxynonenal (4-HNE; red) show increased ferroptosis in kidneys from mice with alpha myeloperoxidase (α MPO)-induced necrotizing crescentic glomerulonephritis (AAV) compared with control mice (Ctrl). CD31 (green) was used to stain endothelial cells and 4',6-diamidino-2-phenylindole (DAPI; blue) to stain nuclei. Selected glomeruli in upper panels (original magnification $\times 20$) were enlarged. Bar = 50 μ m. (b) Acyl-CoA synthetase long chain family member 4 (ACSL4) and (c) glutathione peroxidase 4 (GPX4) protein expression were determined in kidney lysates from mice with α MPO AAV by western blot. Healthy mice were used as control (Ctrl). β -Actin was used as loading control. The respective quantification shows an increased ACSL4 ($n = 4$) and a decreased GPX4 expression ($n = 8-9$) in AAV mice. (d) *Acsl4* and (e) *Gpx4* mRNA expression were determined by reverse transcriptase-polymerase chain reaction in kidney lysates from AAV and control mice. Error bars indicate means \pm SEM. * $P < 0.05$; *** $P < 0.001$. To optimize viewing of this image, please see the online version of this article at www.kidney-international.org.

whether Fer-1 might directly modulate CD4⁺ T-cell proliferation and polarization. Murine CD4⁺ cells isolated from

spleens were labeled with carboxyfluorescein succinimidyl ester and incubated with CD3/CD28 Dynabeads, and

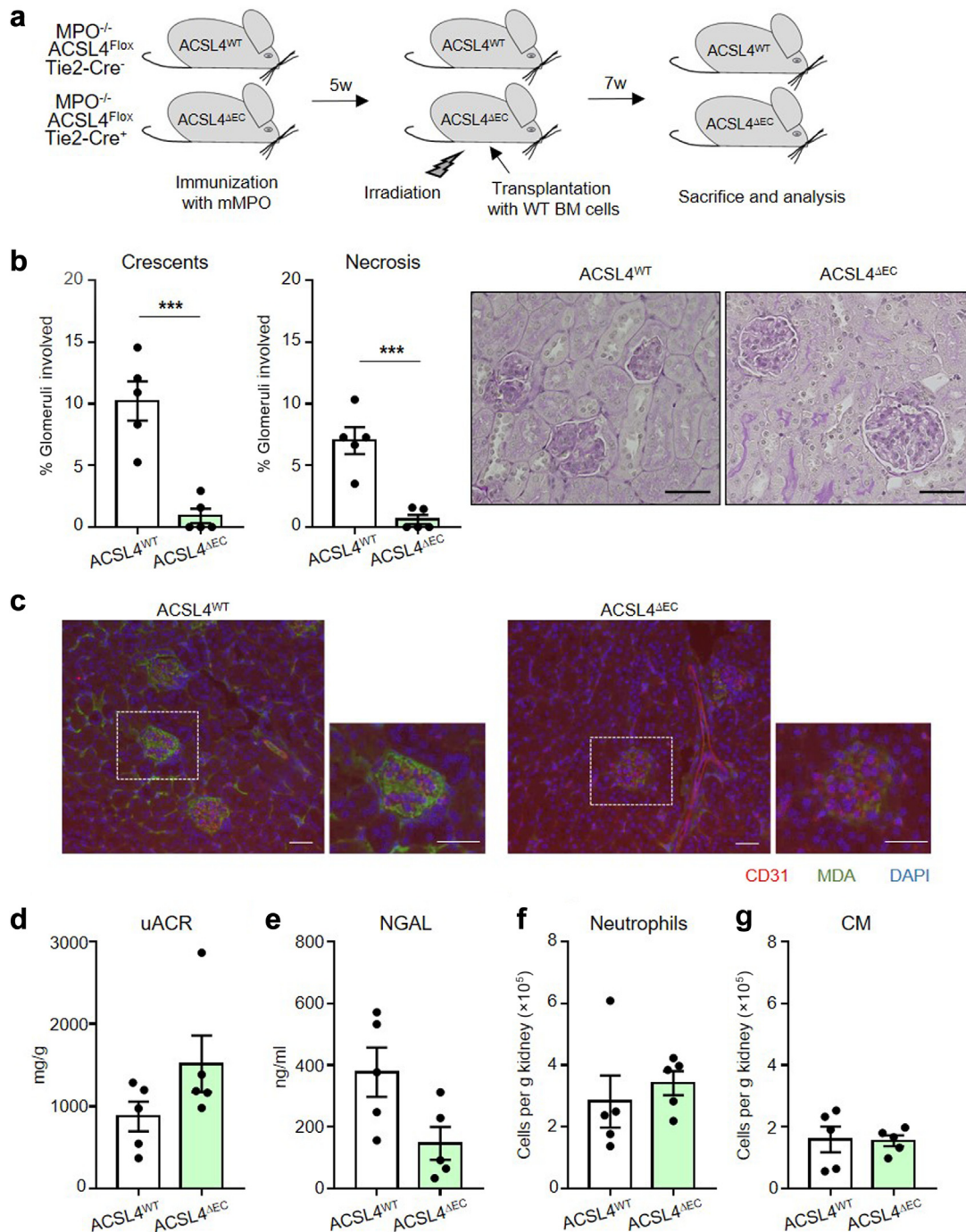


Figure 5 | Chimeric mice lacking acyl-CoA synthetase long chain family member 4 (ACSL4) in endothelial cells (ECs) are protected from anti-myeloperoxidase (anti-MPO) IgG-induced necrotizing crescentic glomerulonephritis (NCGN). (a) Experimental settings describing the induction of NCGN in MPO^{-/-}ACSL4^{Flox}Tie2-Cre⁻ mice with a normal ACSL4 expression (ACSL4^{WT}) and in MPO^{-/-}ACSL4^{Flox}Tie2-Cre⁺ mice with an EC-specific ACSL4 deletion (ACSL4^{ΔEC}). (b) Mice with a specific ACSL4 deletion in ECs developed less renal damage with a reduction of crescentic and necrotic glomeruli compared with control mice. A representative image of a kidney section stained with periodic acid-Schiff at high magnification (original magnification ×20) is shown for each group. Bar = 50 μm. (c) Representative immunofluorescence images (original magnification ×20) for malondialdehyde (MDA; green) show reduced ferroptosis in kidneys from ACSL4^{ΔEC} mice. CD31 (red) was used to stain ECs and 4',6-diamidino-2-phenylindole (DAPI; blue) to stain nuclei. Bar = 50 μm. (d) Urine albumin-creatinine ratio (uACR) and (e) neutrophil gelatinase-associated lipocalin (NGAL) urine levels determined by enzyme-linked immunosorbent assay (ELISA) were similar for both groups. (f) Renal immune cells were analyzed by flow cytometry. Infiltration of CD11b⁺Ly6G⁺ neutrophils and CD11b⁺Ly6G⁻Ly6C⁺ classical monocytes (CM) was similar in both groups. The number of immune cells is expressed per gram (g) kidney and calculated using counting beads. Error bars indicate means ± SEM. ***P < 0.001. BM, bone marrow; WT, wild type. To optimize viewing of this image, please see the online version of this article at www.kidney-international.org.

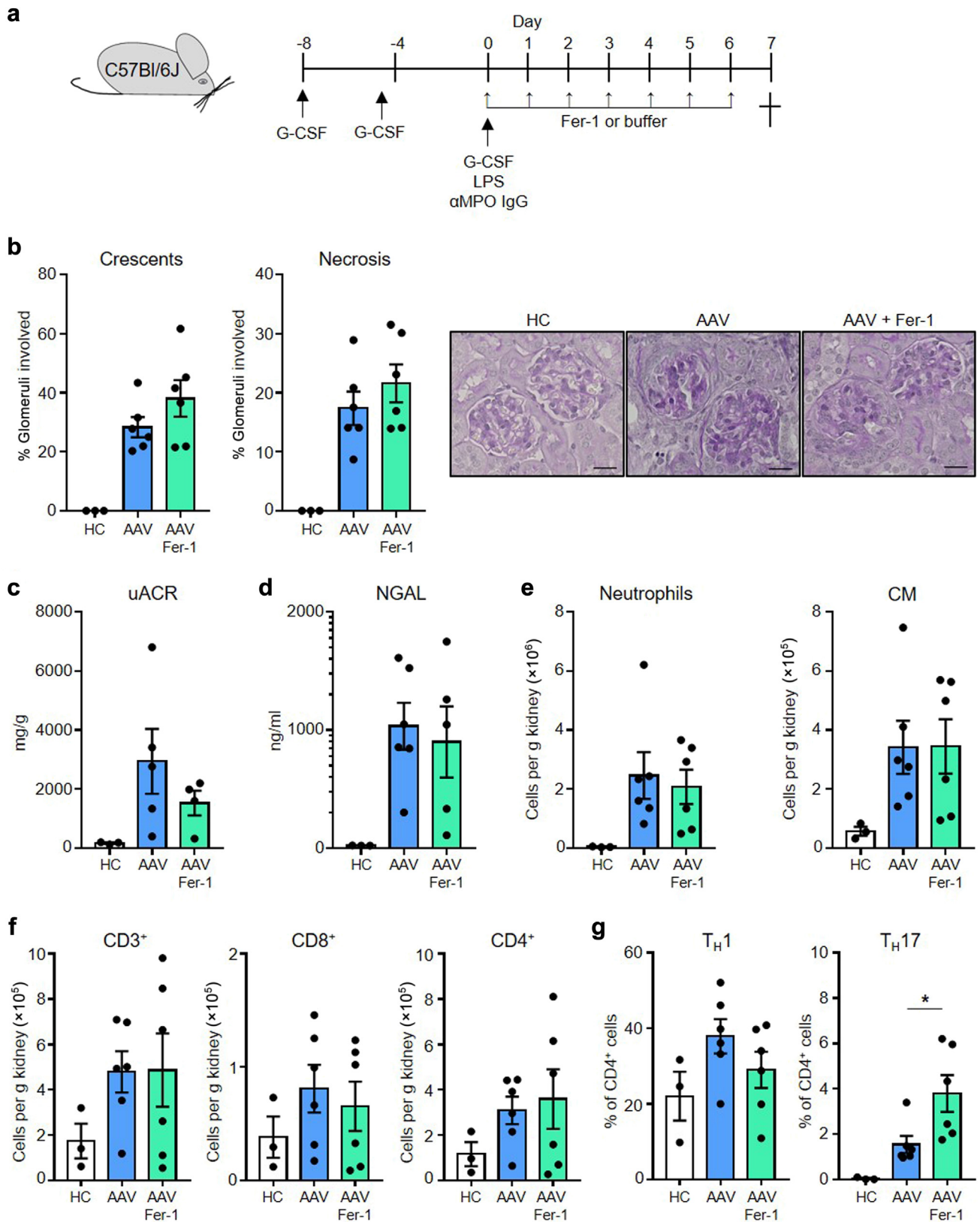


Figure 6 | Ferroptosis inhibition with Ferrostatin-1 (Fer-1) does not protect mice from the development of antineutrophil cytoplasmic antibody (ANCA)-associated necrotizing crescentic glomerulonephritis (NCGN). (a) Experimental settings describing the induction of NCGN in wild-type mice induced by granulocyte colony-stimulating factor (G-CSF; 30 μg/mouse), lipopolysaccharide (LPS; 5 μg/g body weight), and alpha myeloperoxidase (αMPO) IgG (50 μg/g body weight) injection. Ferroptosis inhibition was mediated by daily injection of Fer-1 (3 μg/g body weight) from day 0 until sacrifice at day 7. (b) Mice treated with Fer-1 developed similar renal damage to (continued)

proliferation was analyzed by flow cytometry. For the polarization assay, sorted cells were incubated in T_H17 polarizing medium for 6 days and $IL17^+$ cells were quantified by flow cytometry. We observed a direct positive impact of Fer-1 treatment on $CD4^+$ cell proliferation but not on polarization (Figure 7b and c). Next, we investigated whether Fer-1 would indirectly modulate T-cell functions by interfering with myeloid cells such as monocytes. To test this hypothesis, we generated cf-SN from anti-MPO IgG-stimulated murine monocytes preincubated with Fer-1 or buffer control. Supernatants from monocytes stimulated with tumor necrosis factor- α alone or unstimulated were used as control. cf-SN from anti-MPO IgG-treated monocytes that were preincubated with Fer-1, but not with buffer control, significantly increased $CD4^+$ proliferation and polarization (Figure 7d and e). This effect was not seen when monocytes were preincubated with Fer-1 or treated with isotype control or left untreated. These data suggest that Fer-1 modulates monocyte proinflammatory functions that in turn modulate T cells in a paracrine fashion. For instance, we observed that Fer-1 treatment slightly, albeit significantly, decreased $IL-1\beta$ release in α MPO IgG-stimulated monocytes (Supplementary Figure S5A). It is unlikely that these effects played a role as $IL-1\beta$ is a key factor for T_H17 polarization. Fer-1 treatment had no effect on $IL-6$ release (Supplementary Figure S5A). Studying Fer-1 effects on murine neutrophil functions, we observed that preincubation with Fer-1 significantly increased ANCA-stimulated NET generation in neutrophils isolated from the bone marrow (Figure 7f). We observed similar effects in human neutrophils isolated from the blood (Supplementary Figure S5B).

Together, these findings indicate that ferroptosis inhibition leads both directly to stimulation of T-cell proliferation and indirectly to myeloid cell-mediated paracrine T-cell proliferation as well as T_H17 cell polarization (Figure 6g). These effects are important disease mediators in AAV and likely counteract the beneficial effects of ferroptosis inhibition in other renal and vascular cells such as ECs.

DISCUSSION

Our study revealed important novel findings with potential clinical implications. First, ferroptosis provides the major cell death pathway in vascular endothelium challenged by ANCA-activated neutrophils. Second, we demonstrate that EC ferroptosis is increased in kidneys from mice with AAV and that mice lacking ACSL4 specifically in EC were protected from

the development of anti-MPO IgG-induced NCGN. Third, in contrast to genetic deletion in EC, we report that systemic ferroptosis inhibition with Fer-1 or Liprox-1 did not protect mice from NCGN and therefore does not provide a promising therapeutic option for patients with AAV. Fourth, we observed that pharmacologic ferroptosis inhibition with Fer-1 promoted proinflammatory functions of myeloid cells, namely monocyte-mediated T_H17 polarization and NET production. These effects counteract the beneficial effect of ferroptosis inhibition in EC and may explain the lack of renal protection with systemic Fer-1 treatment in AAV.

EC damage leads to vascular and renal cell necrosis during AAV. Neutrophils and monocytes are important mediators of this injury process.⁴ It has been shown that necrosis is regulated by distinct regulated cell death pathways, including necroptosis, pyroptosis, and ferroptosis.⁸ These pathways, essential for tissue homeostasis, have been increasingly reported to be important in inflammatory process and disease development.¹⁹ Ferroptosis is driven by oxidative stress and iron-dependent phospholipid peroxidation,¹⁰ which makes it an attractive hypothetical target in AAV-mediated vascular damage. We provide evidence that supernatants from ANCA-activated neutrophils induced lipid peroxidation and subsequent EC death that was reduced by ferroptosis inhibition with Fer-1 or Liprox-1 but not by compounds blocking either necroptosis or apoptosis. A second approach, namely downregulation of the central ferroptosis mediator ACSL4 with siRNA, recapitulated the effect of Fer-1 and Liprox-1 treatment. Several factors released from ANCA-activated neutrophils have been implicated as mediators of EC injury, including microparticles,²⁰ neutrophil serine proteases,⁶ NETs,⁷ and MPO.²¹ Whether 1 or more of these mediators modulate ferroptosis in EC should be explored in future studies.

Using a preclinical AAV model, we detected several ferroptosis markers that were increased in kidneys from AAV compared with healthy mice. Increased lipid peroxidation was found in glomerular and extraglomerular vessels. In addition, ACSL4, an enzyme promoting lipid peroxidation, was increased at mRNA and protein levels. In contrast, GPX4 that protects cells from peroxidation was downregulated. These data indicate locally activated EC ferroptosis in kidneys during AAV. Based on these findings, we investigated whether EC ferroptosis contributes to NCGN in a murine AAV model. We generated mice with an EC-specific ACSL4 deletion that were protected from anti-MPO IgG-induced NCGN. This

Figure 6 | (continued) mice without treatment. Representative images of kidney sections stained with periodic acid-Schiff at high magnification (original magnification $\times 40$) and quantitative analyses of glomeruli with crescents and necrosis are shown for each group. Bar = 20 μ m. Data from 3 healthy mice are provided for comparison. (c) Urine albumin-creatinine ratio (uACR) and (d) neutrophil gelatinase-associated lipocalin (NGAL) urine levels determined by enzyme-linked immunosorbent assay were similar in both groups. (e) Myeloid cell infiltration was analyzed by flow cytometry. Infiltration of $CD11b^+Ly6G^+$ neutrophils and $CD11b^+Ly6G^-Ly6C^+$ classical monocytes (CM) was similar in both groups. (f) Lymphoid cell infiltration was analyzed by flow cytometry. Infiltration of $CD3^+$, $CD4^+$, and $CD8^+$ cells (per gram kidney) was similar in both groups. (g) T helper cell (T_H)1 and T_H17 cell subsets were determined by flow cytometry and expressed as percentage of $CD4^+$ cells. T_H17 cells were increased in mice treated with Fer-1. The number of immune cells expressed per gram (g) kidney was calculated using counting beads. Error bars indicate means \pm SEM. * $P < 0.05$. AAV, antineutrophil cytoplasmic antibody-associated vasculitis; HC, healthy control; LPS, lipopolysaccharide. To optimize viewing of this image, please see the online version of this article at www.kidney-international.org.

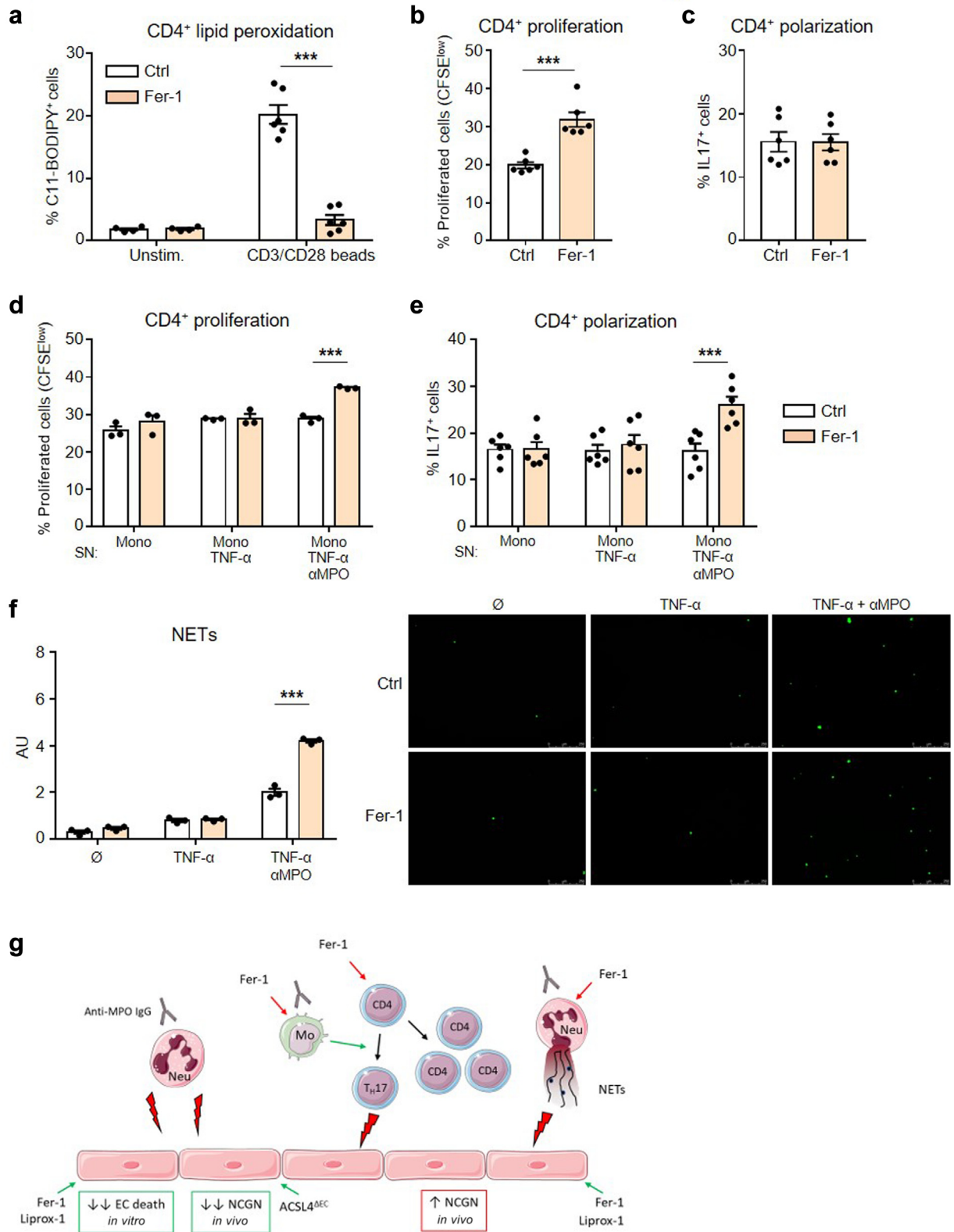


Figure 7 | Ferrostatin-1 (Fer-1) increases monocyte-mediated T-cell polarization, proliferation, and neutrophil extracellular trap (NET) release *in vitro*. (a) CD4⁺ T cells isolated from spleens of C57Bl/6J mice were incubated with CD3/CD28 Dynabeads (at a bead/cell ratio of 1:2.5). After 3 days, cells were washed with phosphate-buffered saline, collected with trypsin, stained with C11-BODIPY 581/591, and analyzed by flow cytometry (duplicates from 3 independent experiments). (b) CD4⁺ T cells isolated from spleens of C57Bl/6J mice were labeled with carboxyfluorescein succinimidyl ester (CFSE) and incubated with CD3/CD28 Dynabeads (at a bead/cell ratio of 1:2.5). Fer-1 was used to inhibit ferroptosis. After 72 hours in culture, proliferation was assessed by flow cytometry. The corresponding percentages of (continued)

beneficial effect was not explained by reduced myeloid cell infiltration as renal neutrophil and classical monocyte numbers were similar in both groups. However, we observed decreased lipid peroxidation in kidneys from ACSL4^{ΔEC} mice.

One might speculate that ferroptosis-deficient ECs modulate the immune response to necrosis, a process defined as necroinflammation.²² Increasing evidence suggests that EC ferroptosis is widely involved in multiple vascular diseases including atherosclerosis and ischemia/reperfusion injury.²³ Moreover, ferroptosis was associated with tubular cell death in different models of AKI.²⁴ Mice lacking ACSL4 specifically in tubular cells showed reduced ferroptosis and renal injury after ischemia/reperfusion-induced AKI.²⁵ Studies have demonstrated that iron chelators and specific ferroptosis inhibitors had protective effects in various AKI animal models.^{26,27} Based on these reports from the literature and our observation from ACSL4^{ΔEC} mice, we hypothesized that systemic ferroptosis inhibition with the small compound Fer-1 would protect mice from anti-MPO IgG-induced NCGN. However, in contrast to our expectation, systemic Fer-1 or Liprox-1 treatment had no beneficial therapeutic effect. Kidney damage, myeloid cell infiltration, and lipid peroxidation were similar in treated and untreated mice.

We explored mechanisms explaining the discrepancy between EC-specific and systemic ferroptosis inhibition. We studied the effects of pharmacologic ferroptosis inhibition on immune cells that may counteract the beneficial effect of endothelial ferroptosis inhibition. For instance, several observations suggested that the activity and function of CD4⁺ helper T cells are regulated by ferroptosis.²⁸ We found that renal T_H17 cells were increased in AAV mice systemically treated with Fer-1. Whereas Fer-1 did affect only CD4⁺ T-cell proliferation directly, Fer-1 increased the capacity of ANCA-activated monocytes to promote CD4⁺ proliferation and T_H17 polarization. This finding explains, at least in part, the lack of protection from NCGN in Fer-1-treated mice because we and others established that T_H17 cells are important disease mediators in AAV.^{29–32}

We also found that Fer-1 had a direct immunomodulatory influence on neutrophils. Indeed, ferroptosis inhibition with Fer-1 increased the release of NETs, whereas ferroptosis activation with the RSL3 compound completely inhibited NET production (data not shown). Thus, a possible crosstalk between ferroptosis and necroptosis might be involved in neutrophils with ferroptosis inhibition potentially accelerating necroptosis. Such concept that ferroptosis and necroptosis are not only interconnected but also are alternative to one another in ischemia/reperfusion-induced AKI has been recently reported.³³ This finding may provide an additional explanation for the lack of renal protection in AAV mice systemically treated with Fer-1 because some studies showed previously that NET generation promotes NCGN in AAV.^{7,34} Consequently, our observations raise the possibility that dual necroptosis/ferroptosis inhibition, rather than ferroptosis inhibition alone, might represent a promising therapeutic strategy in AAV. The potential links between ferroptosis and necroptosis in neutrophils and AAV remain to be confirmed in additional studies.

Our study has some limitations. Although our study focuses on EC, we cannot exclude that ferroptosis is not increased in other renal cells such as glomerular and tubular cells. Single-cell experiments might be helpful to better define a ferroptosis signature in different renal cell populations. Ferroptosis inhibition was tested in a more severe, short-term AAV model, whereas the protective effects of *Acs4* genetic deletion in EC was observed in our bone marrow model. Daily Fer-1 and Liprox-1 i.p. injections represent a burden for mice and therefore are difficult to apply over several weeks. Specific oral ferroptosis inhibitors that could be used in the bone marrow model are currently not available. Finally, it is not excluded that other compounds interfering with ferroptosis such as iron chelators might represent alternative strategies.

In conclusion, we have characterized that ANCA-activated neutrophils induce ferroptosis in EC. ACSL4 genetic deletion in EC protected mice from the development of NCGN in

Figure 7 | (continued) proliferated cells are shown (duplicates from 3 independent experiments). (c) Isolated CD4⁺ T cells from spleens of C57Bl/6J mice were incubated with CD3/CD28 Dynabeads (at a bead/cell ratio of 1:1) in T helper cell (T_H)17 polarization medium for 6 days and analyzed by flow cytometry. Fer-1 was used to inhibit ferroptosis. Percentages of T_H17 T cells (interleukin-17A [IL-17A]⁺ interferon-γ [IFNγ]⁺) are shown (duplicates from 3 independent experiments). (d) CD4⁺ T cells isolated from spleens of C57Bl/6J mice were labeled with CFSE and incubated with CD3/CD28 Dynabeads (at a bead/cell ratio of 1:2.5) in the presence of the indicated cell-free supernatants (cf-SN) from monocytes. Monocytes isolated from the bone marrow were primed with tumor necrosis factor-α (TNF-α) for 15 minutes and further stimulated with anti-myeloperoxidase (anti-MPO) IgG for 4 hours. In respective conditions, cells were preincubated with Fer-1 for 30 minutes. cf-SN from unstimulated monocytes were used as control. All cf-SN were obtained by centrifugation and added at day 0 to CD4⁺ cells (at a monocyte/CD4⁺ cell ratio of 5:1). After 72 hours in culture, proliferation was assessed by flow cytometry. The corresponding percentages of proliferated cells are shown (n = 3). (e) Isolated CD4⁺ T cells from spleens of C57Bl/6J mice were incubated with CD3/CD28 Dynabeads (at a bead/cell ratio of 1:1) in T_H17 polarization medium in the presence of cf-SN from monocytes (at a monocyte/CD4⁺ cell ratio of 5:1) for 6 days and analyzed by flow cytometry. cf-SN were added at day 0 and day 3. Percentages of T_H17 T cells (IL-17A⁺IFNγ⁺) are shown (duplicates from 3 independent experiments). (f) Isolated mouse neutrophils were primed with TNF-α for 15 minutes and subsequently stimulated with either TNF-α alone or anti-MPO IgG for 4 hours. In some conditions, cells were pretreated with Fer-1 for 30 minutes. Viable cells were stained with SYTOX green to detect NETs by microscopy (original magnification ×20). The corresponding statistical analysis of the amount of SYTOX green positive area (NET-producing neutrophils) expressed as arbitrary unit (AU) from 3 independent experiments with different neutrophil donors is shown. (g) Cartoon representing the effect of genetic and chemical ferroptosis inhibition on endothelial, myeloid, and T cells *in vitro* and *in vivo*. Error bars indicate means ± SEM. ***P < 0.001. EC, endothelial cell; Unstim, unstimulated. Parts of panel (g) were drawn by using pictures provided by Servier Medical Art (Servier; <https://smart.servier.com>), licensed under a Creative Commons Attribution 4.0 Unported License. To optimize viewing of this image, please see the online version of this article at www.kidney-international.org.

AAV and therefore confirmed an important role of EC ferroptosis for the development of NCGN-associated AAV. In contrast, systemic ferroptosis inhibition with 2 different compounds did not provide any benefice to mice with AAV. Therefore, ferroptosis inhibition alone should not be considered as a potential new therapeutic strategy for AAV patients.

DISCLOSURE

All the authors declared no competing interests.

DATA STATEMENT

The authors confirm that the data supporting the findings of this study are available in the article and its supplementary materials. The custom resources related to the article are available from the corresponding authors upon request. This article does not report large datasets, original code, or reanalyzed data.

ACKNOWLEDGMENTS

We thank Professor A. Linkermann, Division of Nephrology, Department of Internal Medicine III, University Hospital Carl Gustav Carus at the Technische Universität Dresden, Germany, for helpful discussion and input on the project. We also thank Sylvia Lucke, Susanne Rolle, and Tanja Filipowski for excellent technical assistance. This work was supported by grants SCHR 771/10-1 and SCHR 771/8-1 from the Deutsche Forschungsgemeinschaft to AS, grant 394046635-SFB 1365 from the Deutsche Forschungsgemeinschaft to RK and AS, and Experimental and Clinical Research Center (ECRC) grants to AS and RK. Parts of the visual abstract, [Figure 7g](#), and [Supplementary Figure S1](#) were drawn by using pictures provided by Servier Medical Art (Servier; <https://smart.servier.com>), licensed under a Creative Commons Attribution 4.0 Unported License.

AUTHOR CONTRIBUTIONS

AR, RK, and AS designed the study; AR, JS, DL, LK, JS, and AS carried out experiments; AR and AS analyzed the data; A.R and AS generated the figures; AR, RK, and AS drafted the manuscript; and all authors revised the paper and approved the final version of the manuscript.

Supplementary material is available online at www.kidney-international.org.

REFERENCES

- Falk RJ, Jennette JC. Anti-neutrophil cytoplasmic autoantibodies with specificity for myeloperoxidase in patients with systemic vasculitis and idiopathic necrotizing and crescentic glomerulonephritis. *N Engl J Med*. 1988;318:1651–1657.
- Van Der Woude FJ, Lobatto S, Permin H, et al. Autoantibodies against neutrophils and monocytes: tool for diagnosis and marker of disease activity in Wegener's granulomatosis. *Lancet*. 1985;325:425–429.
- Kitching AR, Anders HJ, Basu N, et al. ANCA-associated vasculitis. *Nat Rev Dis Primer*. 2020;6:71.
- Jennette JC, Falk RJ. Pathogenesis of antineutrophil cytoplasmic autoantibody-mediated disease. *Nat Rev Rheumatol*. 2014;10:463–473.
- Massicotte-Azarniouch D, Herrera CA, Jennette JC, et al. Mechanisms of vascular damage in ANCA vasculitis. *Semin Immunopathol*. 2022;44:325–345.
- Jerke U, Hernandez DP, Beaudette P, et al. Neutrophil serine proteases exert proteolytic activity on endothelial cells. *Kidney Int*. 2015;88:764–775.
- Schreiber A, Rousselle A, Becker JU, et al. Necroptosis controls NET generation and mediates complement activation, endothelial damage, and autoimmune vasculitis. *Proc Natl Acad Sci*. 2017;114:E9618–E9625.
- Tang D, Kang R, Berghe TV, et al. The molecular machinery of regulated cell death. *Cell Res*. 2019;29:347–364.
- Linkermann A, Green DR. Necroptosis. *N Engl J Med*. 2014;370:455–465.
- Dixon SJ, Lemberg KM, Lamprecht MR, et al. Ferroptosis: an iron-dependent form of nonapoptotic cell death. *Cell*. 2012;149:1060–1072.
- Doll S, Proneth B, Tyurina YY, et al. ACSL4 dictates ferroptosis sensitivity by shaping cellular lipid composition. *Nat Chem Biol*. 2017;13:91–98.
- Kagan VE, Mao G, Qu F, et al. Oxidized arachidonic and adrenic PEs navigate cells to ferroptosis. *Nat Chem Biol*. 2017;13:81–90.
- Yang WS, SriRamaratnam R, Welsch ME, et al. Regulation of ferroptotic cancer cell death by GPX4. *Cell*. 2014;156:317–331.
- Stockwell BR. Ferroptosis turns 10: emerging mechanisms, physiological functions, and therapeutic applications. *Cell*. 2022;185:2401–2421.
- Linkermann A, Skouta R, Himmerkus N, et al. Synchronized renal tubular cell death involves ferroptosis. *Proc Natl Acad Sci U S A*. 2014;111:16836–16841.
- Martin-Sanchez D, Ruiz-Andres O, Poveda J, et al. Ferroptosis, but not necroptosis, is important in nephrotoxic folic acid-induced AKI. *J Am Soc Nephrol*. 2017;28:218–229.
- Li P, Jiang M, Li K, et al. Glutathione peroxidase 4-regulated neutrophil ferroptosis induces systemic autoimmunity. *Nat Immunol*. 2021;22:1107–1117.
- Schreiber A, Xiao H, Falk RJ, Jennette JC. Bone marrow-derived cells are sufficient and necessary targets to mediate glomerulonephritis and vasculitis induced by anti-myeloperoxidase antibodies. *J Am Soc Nephrol*. 2006;17:3355–3364.
- Tonnus W, Meyer C, Paliege A, et al. The pathological features of regulated necrosis. *J Pathol*. 2019;247:697–707.
- Hong Y, Eleftheriou D, Hussain AAK, et al. Anti-neutrophil cytoplasmic antibodies stimulate release of neutrophil microparticles. *J Am Soc Nephrol*. 2012;23:49–62.
- Antonelou M, Michaëlsson E, Evans RDR, et al. Therapeutic myeloperoxidase inhibition attenuates neutrophil activation, ANCA-mediated endothelial damage, and crescentic GN. *J Am Soc Nephrol*. 2020;31:350–364.
- Sarhan M, Land WG, Tonnus W, Hugo CP, Linkermann A. Origin and consequences of necroinflammation. *Physiol Rev*. 2018;98:727–780.
- Zhang H, Zhou S, Sun M, et al. Ferroptosis of endothelial cells in vascular diseases. *Nutrients*. 2022;14:4506.
- Li J, Cao F, Yin HL, et al. Ferroptosis: past, present and future. *Cell Death Dis*. 2020;11:88.
- Wang Y, Zhang M, Bi R, et al. ACSL4 deficiency confers protection against ferroptosis-mediated acute kidney injury. *Redox Biol*. 2022;51:102262.
- Skouta R, Dixon SJ, Wang J, et al. Ferrostatins inhibit oxidative lipid damage and cell death in diverse disease models. *J Am Chem Soc*. 2014;136:4551–4556.
- Feng Q, Yu X, Qiao Y, et al. Ferroptosis and acute kidney injury (AKI): molecular mechanisms and therapeutic potentials. *Front Pharmacol*. 2022;13:858676.
- Chen X, Kang R, Kroemer G, Tang D. Ferroptosis in infection, inflammation, and immunity. *J Exp Med*. 2021;218:e20210518.
- Gan PY, Steinmetz OM, Tan DSY, et al. Th17 cells promote autoimmune anti-myeloperoxidase glomerulonephritis. *J Am Soc Nephrol*. 2010;21:925–931.
- Steinmetz OM, Summers SA, Gan PY, et al. The Th17-defining transcription factor ROR γ t promotes glomerulonephritis. *J Am Soc Nephrol*. 2011;22:472–483.
- Schreiber A, Rousselle A, Klocke J, et al. Neutrophil gelatinase-associated lipocalin protects from ANCA-induced GN by inhibiting TH17 immunity. *J Am Soc Nephrol*. 2020;31:1569–1584.
- Rousselle A, Sonnemann J, Amann K, et al. CSF2-dependent monocyte education in the pathogenesis of ANCA-induced glomerulonephritis. *Ann Rheum Dis*. 2022;81:1162–1172.
- Müller T, Dewitz C, Schmitz J, et al. Necroptosis and ferroptosis are alternative cell death pathways that operate in acute kidney failure. *Cell Mol Life Sci*. 2017;74:3631–3645.
- Kessenbrock K, Krumbholz M, Schönemmarck U, et al. Netting neutrophils in autoimmune small-vessel vasculitis. *Nat Med*. 2009;15:623–625.